Received: 23 October 2020 | Revised: 29 January 2021 | Accepted: 2 February 2021

DOI: 10.1002/dep2.139

ORIGINAL RESEARCH ARTICLE

The Depositional Record Open Access
A journal of the International Association of Sedimentologists
WILEY

# Taking the heat out of British Jurassic septarian concretions

**Richmal B. Paxton**[1] | **Paul F. Dennis**[1] | **Alina D. Marca**[1] | **James P. Hendry**[2] | **John D. Hudson**[3] | **Julian E. Andrews**[1]

[1]School of Environmental Sciences, University of East Anglia, Norwich, UK

[2]Iapetus Geoscience Limited, Greystones, Co. Wicklow, Ireland

[3]School of Geography, Geology and Environment, University of Leicester, Leicester, UK

**Correspondence**
Richmal B. Paxton, School of Environmental Sciences, University of East Anglia, Norwich, NR4 7TJ, UK.
Email: r.paxton@uea.ac.uk

**Funding information**
Natural Environment Research Council, Grant/Award Number: NE/L002582/1

## Abstract

Septarian carbonate concretions in marine mudrocks contain calcite cements that should represent evolving conditions from ambient temperature, shallow subsurface environments to warmer, burial diagenetic conditions. Clumped isotope results from British Middle and Upper Jurassic concretions indicate that most concretion body calcites formed at temperatures between 9 ± 5°C and 18 ± 5°C from marine pore waters with $\delta^{18}O$ values between 0.2 ± 1.1‰ and −2.2 ± 1.1‰$_{VSMOW}$. Early diagenetic, brown, fibrous calcite fracture cements mostly formed at temperatures between 15 ± 5°C and 19 ± 5°C, again from marine-derived pore fluids with $\delta^{18}O$ compositions between −0.5 ± 1.1‰ and 0.3 ± 1.2‰$_{VSMOW}$. Two of these cements showed evolution to warmer temperatures and more evolved pore fluids with growth, indicating transition to deeper burial conditions. Later diagenetic, sparry calcite cements gave more variable temperatures but all indicated involvement of meteoric pore fluids. The highest clumped isotope temperature (43 ± 6°C) is within error of the 50°C regional maximum burial temperature estimate. These results are consistent with published geological and stable isotope constraints on the formation of Jurassic septarian concretions and highlight their potential as robust archives of marine benthic palaeotemperatures. Some of these results differ from clumped isotope data in an earlier study that reported higher temperatures for concretion body and early diagenetic fibrous cement fringes probably due to methodological differences.

**KEYWORDS**

carbonate cements, clumped isotopes, Jurassic, palaeotemperature, septarian concretions

## 1 | INTRODUCTION

There is considerable interest in the application of clumped isotope palaeothermometry for reconstructing temperatures from carbonate rocks and fossils from a range of Earth surface palaeoenvironmental and diagenetic settings (Eiler, 2007, 2011; Ghosh et al., 2006; Huntington et al., 2011). While clumped isotope palaeothermometry does not require prior assumptions regarding temperature or water isotopic compositions, a potential drawback is that many Earth surface biotic and abiotic carbonates probably crystallize too rapidly to achieve the complete isotopic equilibrium (Daëron et al., 2019) required to apply the technique quantitatively. This said, some abiotic carbonates, particularly slowly growing sparry calcite cements in basinal sediments, should be excellent targets for clumped isotope analysis. These sparry cements typically formed under shallow to deep burial conditions where warmer temperatures (e.g. 20–50°C; Defliese &

Lohmann, 2016; Purvis et al., 2020) ensure isotope exchange reaction rates are fast, and dissolved inorganic carbon (DIC)-calcite equilibrium is probably achieved.

Ancient carbonate concretions (Raiswell & Fisher, 2000) are obvious targets for clumped isotope palaeothermometry and the first $\Delta_{47}$ data (Loyd et al., 2012) showed that concretion body cements were influenced by post-depositional fluid alteration, driven by either silica diagenesis (Miocene, Monterey Formation) or meteoric water influx (Cretaceous Holz Shale Formation).

This study was followed by clumped isotope palaeothermometry on septarian concretions (Dale et al., 2014; Loyd et al., 2014) of various ages, attractive targets because a single decimetre-sized concretion can contain a variety of carbonate cements that record changes in the geochemical environment and temperature from initial formation through progressive burial in sedimentary basins over millions of years. Both studies reconstructed cementation temperatures and the fluid types involved in concretion cementation. Their results showed that some concretion bodies gave temperatures indicative of formation at shallow depths (Loyd et al., 2014), while other concretion body data indicated much higher temperatures (Dale et al., 2014; Loyd et al., 2014), apparently resolving some of the uncertainty inherent in traditional stable isotope data (Mozley & Burns, 1993). However, clumped isotope palaeothermometry is not a panacea; each case study needs careful evaluation of all supporting data. For example, clumped isotope data show that negative $\delta^{18}O$ values in sparry calcite cements filling septarian fractures may not indicate meteoric water input (Dale et al., 2014), although they often do (Loyd et al., 2014).

This study concentrates on British Jurassic concretions, which have a history of detailed previous research (Hendry et al., 2006; Hudson, 1978; Hudson et al., 2001) allowing the new clumped isotope information to be constrained in a tight framework of supporting data. These Jurassic concretions are thought to have formed in unconsolidated, organic-rich, marine muds (Duff, 1975; Kenig et al., 1994) within a few metres of the sea floor (Hendry et al., 2006; Hudson, 1978). Concretion bodies (Figure 1) may have initiated from a biomineralization of a bacterial extra-cellular polysaccharide framework (Hendry et al., 2006) which was rapidly entombed by microsparry calcite cement. The pore water from which this cement precipitated was essentially sea water, while bacterial sulphate reduction (BSR) caused the incorporation of isotopically negative C in calcite, and S in pyrite (De Craen et al., 1999; Irwin et al., 1977).

The lithifying concretion bodies contracted at an early stage of cementation, forming septarian cracks (Figure 1) or more irregular breccias within an otherwise unconsolidated sediment. Mobile clays, intruded into cracks at both Calvert and Staffin (Figure 2), are direct evidence of this, and pyrite coating breccia fragments are evidence this happened in the BSR zone (Hudson, 1978; Hudson et al., 2001). In many cases, brown fibrous cements nucleated on crack walls forming distinct cement fringes (Figure 1).

The Sr isotope compositions of early calcite phases (concretion bodies and fibrous cement fringes) in the English concretions are very close to those of Callovian sea water (Hudson et al., 2001). Moreover, the $\delta^{18}O$ values of these phases are similar to those from well-preserved benthic fossils, which led Hudson et al. (2001) to infer early calcite cementation temperatures of *ca* 15°C, assuming the widely accepted $\delta^{18}O$ composition for Jurassic sea water of $-1‰_{VSMOW}$ (Shackleton & Kennett, 1975). The last stage of concretion development resulted in the precipitation of ferroan sparry calcite in the septaria (Figure 1), cements

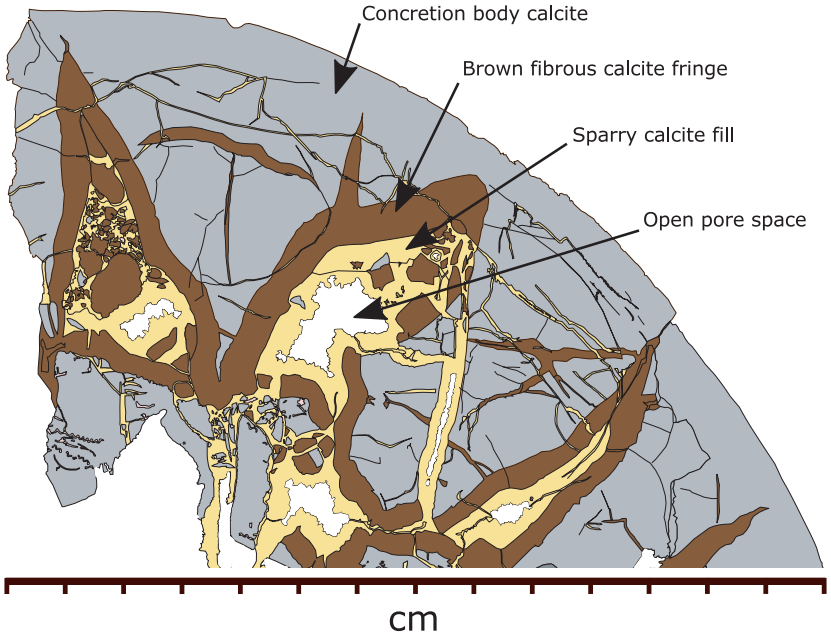


**FIGURE 1** Line drawing from a slab of Staffin Shale Formation concretion showing the various calcite phases described in this paper

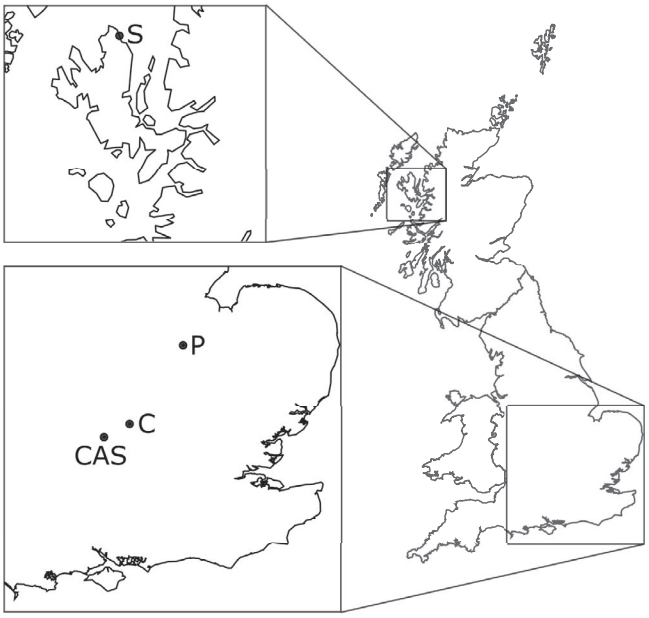


**FIGURE 2** Sample locations. C = Calvert; CAS = Cassington; P = Peterborough; S = Staffin

that have distinctly negative $\delta^{18}O$ values (mean $\delta^{18}O$ of $-7.4‰_{VPDB}$) indicative of a meteoric fluid (Hudson, 1978). Likewise, at Staffin, Hendry et al. (2006) derived minimum concretion body and fibrous calcite cementation temperatures *ca* 10°C, with ferroan sparry calcites displaying a wide range in $\delta^{18}O$ values ascribed to variable mixing of marine and highly $^{18}O$-depleted meteoric pore fluids.

This study is timely because Loyd et al. (2014) reported clumped isotope temperatures from English Jurassic concretion body calcites and brown fibrous cement fringes that were *ca* 20 to 30°C warmer than those inferred from geological and traditional geochemical evidence (Hudson et al., 2001). They resolved the temperature mismatch by suggesting the shallow burial precursor calcites had undergone pervasive reaction with heated basinal fluids with $\delta^{18}O$ compositions around $+3.2‰_{VSMOW}$; a scenario that is the opposite of the typical 'meteoric water alteration pathway' proposed for calcitic concretions based on an ensemble of stable isotope data (Mozley & Burns, 1993).

### 1.1 | Study Materials

Middle and Upper Jurassic concretions were analysed from a range of localities (Figure 2) and stratigraphic horizons as indicated by ammonites in the concretions (see Cox et al., 1994). These included concretions from brick pits (now back-filled) at Calvert (Jason Subzone, Jason Zone, middle Callovian, Buckinghamshire), Norman Cross Quarry near Peterborough (Obductum Subzone, Coronatum Zone, middle Callovian, Cambridgeshire) and a former gravel pit at Cassington (Obductum Subzone, Coronatum Zone, middle Callovian, Oxfordshire) all described in Hudson (1978) and Hudson et al. (2001). An ex situ concretion derived from the Ampthill Clay (Serratum Subzone, Serratum Zone, upper Oxfordian) was collected from Pleistocene till at Norman Cross quarry (Hudson, 1978). The lower Kimmeridgian Staffin Shale Formation concretions (Densicostata/Normandia Subzone, Baylei Zone) are from the Hebridean Isle of Skye (Hendry et al., 2006). Equivalence of material sampled in earlier published research is in the Supplemental information section 2.

## 2 | METHODS

### 2.1 | Sample preparation

Sample powders from concretion body cements, brown fibrous fringes and void-filling spars were either drilled from cut slices, or produced by crushing fragments (broken from hand specimen) in a pestle and mortar. In all cases areas of sample with visible microfractures or other obvious inhomogeneities were avoided. For three concretions where brown fibrous fringes were >4 mm thick sub-samples were obtained by drilling two trenches (1 mm wide × 1.5 mm deep × 15–20 mm long), one parallel to the inner margin adjacent to the concretion body, and another parallel to the outer margin close to the contact with the succeeding sparry calcite cement.

Sample powders (*ca* 4–6 mg) were reacted in vacuo at 87°C for 30 min with 102% ortho-phosphoric acid in a common acid bath, dynamically collecting the evolved $CO_2$ by freezing into a spiral trap immersed in liquid nitrogen (−196°C). Next the trap was isolated from the reaction vessel, keeping it immersed in liquid nitrogen whilst removing non-condensable gases by vacuum pumping. Then, warming the trap to −120°C, the $CO_2$ was sublimated at low pressure, cryodistilling it into a manometer via two further water traps also held at −120°C. After carrying out a second step of removing non-condensable gas, the gas amount was measured (see Data File S1) to estimate reaction yield. In the last stages of gas purification, the $CO_2$ was transferred through a static porapak-Q trap (120 mm long × 9 mm diameter) held at −20°C, freezing it into a cold finger for 30 min before a final step of removing non-condensable gas.

### 2.2 | Measurement and data handling

Sample $CO_2$ was analysed for $\delta^{45}$-$\delta^{49}$ on the MIRA dual-inlet isotope ratio mass spectrometer (IRMS) using the operating and data handling protocol detailed in Dennis et al. (2019). Samples of the carbonate standards ETH1, ETH3 and ueacmst were prepared and measured each day in order to: (a) determine the transfer function between the local reference frame and the carbon dioxide equilibrium scale (CDES;

Bernasconi et al., 2018), and; (b) to provide an estimate of long-term measurement uncertainty.

Since $\Delta_{47}$ is determined here by reaction at 87°C a correction factor of 0.062‰ is applied to bring the data into line with reported values determined by reaction at 25°C. This correction factor has been previously calibrated for the reaction systems employed here using standards reacted both offline at 25°C and in the present system at 87°C (Supplemental information, section 4).

Further details about methodology, including data reduction, linearity and $^{17}O$ correction are included in the Supplemental information.

## 2.3 | Temperature calculation

The empirical clumped isotope calibration of Kirk (2017) based on measurements made in the UEA laboratory using the MIRA mass spectrometer (Dennis et al., 2019) was used to calculate temperatures:

$$\Delta_{47(\mathrm{ARF})} = \frac{\left(0.0389 \times 10^{6}\right)}{T^{2}} + 0.2139.$$

The calcite-water isotope fractionation factor calibration of Kim and O'Neil (1997), which is appropriate for abiotic carbonates, is used to determine water oxygen isotope compositions.

The isotope values reported here are the mean of 3–6 measurements of replicate samples, with the measurement uncertainty reported as ±1 standard error of the pooled standard deviation of measurements for each of the three phases: concretion bodies, fibrous fringes and spars. In using the pooled standard deviation, it is necessary to ensure that there is a sufficient number of samples to determine a representative distribution of the measurement uncertainty. The standard deviations and errors for 'individual' samples are also reported in the Supplemental Data File. Temperature and fluid isotope compositions are calculated using the mean $\Delta_{47}$ and $\delta^{18}O$ values with full propagation of the measurement and calibration uncertainties. The $\delta^{13}C$ and $\delta^{18}O$ values are reported for carbonates with respect to Vienna-Pee Dee Belemnite (VPDB) and $\delta^{18}O$ values for water with respect to Vienna-standard mean ocean water (VSMOW).

## 2.4 | Sample contexts

The sedimentology, petrography and paragenesis of the various calcites sampled here have been reported before, principally by Hudson (1978) and Hudson et al. (2001; English concretions) and Hendry et al. (2006; Staffin). Salient points are summarised here, discussing published stable isotope data in context with these new data in subsequent sections.

Concretion body calcites are mostly non-ferroan microspars that grew into the pore space of peloidal host sediment. These concretions have pyritic rims consistent with formation in the BSR zone; pyrite formation sequestered available $Fe^{2+}$ explaining the low iron content in the microspars. The Ampthill Clay and Staffin concretions are different; in these the body microspars are ferroan, and the concretions lack pyritic rims. The ferroan composition indicates availability of excess $Fe^{2+}$ for incorporation into calcite either from; (a) iron-reduction under sub-oxic conditions while rates of BSR (and thus pyrite formation) were low; or (b) from upward diffusion of methanogenic $Fe^{2+}$ when BSR had effectively ceased, the latter implying growth near the base of the BSR zone. The ferroan microspars from Staffin have resultant dull-orange cathodoluminescence (CL).

Brown fibrous cement fringes, oriented normal to septarian fracture walls are best described in the Staffin and Ampthill Clay samples (Hendry et al., 2006; Hudson, 1978), comprising radiating palisades (50 μm wide and up to 5,000 μm long), some with fasicular-optic textures. The brown body colour is imparted by polar organic inclusions (Pearson et al., 2005). The earliest phases of growth (Staffin) are non-ferroan and non-luminescent, becoming dull-orange luminescent distally, then passing into more ferroan compositions with dull brown to very dull brown CL, which is interpreted as evidence of initial sub-oxic conditions resulting from a pause in sedimentation, followed by renewed burial and ingress of methanogenic $Fe^{2+}$. Iron content of the English brown fibrous calcites is similarly variable but has not been studied systematically.

The fracture-hosted sparry cements are variably white or yellow ferroan calcites with dull to very dull brown CL. Crystals are typically 0.5–4 mm in size, variously equant to elongate with steep terminations into open spaces.

# 3 | RESULTS

Stable and clumped isotope results for the calcite phases in the concretions are summarised in Table 1 and Figure 3.

The $\delta^{13}C$ and $\delta^{18}O_{carbonate}$ values (Figure 3A) are broadly consistent with previous data from the same Oxford and Ampthill Clay concretions (Hudson, 1978; Hudson et al., 2001); similarly, the data from newly sampled Staffin Shale concretions (Figure 3B) are mainly comparable to data in Hendry et al. (2006). The clumped isotope data (Table 1) mostly show similar paragenetic trends despite being from different geographic areas and stratigraphic units.

Concretion body cements gave temperatures between 9 ± 5°C and 18 ± 5°C, and pore fluid values between 0.2 ± 1.1‰ and −2.2 ± 1.1‰$_{VSMOW}$, excepting concretion SC8 body which gave a temperature of 23 ± 5°C and a pore fluid value of 1.2 ± 1.0‰$_{VSMOW}$ (Figure 3C).

**TABLE 1** Geochemical data and $\Delta_{47}$ temperatures

| Sample | Phase | *N* | $\delta^{13}C$ (‰, VPDB) | $\delta^{18}O_{Carbonate}$ (‰, VPDB) | $\Delta_{47}$ (CDES)[a] | *T* (°C) | $\delta^{18}O_{Fluid}$ (‰, VSMOW) |
|---|---|---|---|---|---|---|---|
| Staffin Shale Formation, Skye[b] | | | | | | | |
| 151-7 | Body | 3 | −17.47 ± 0.06 | −1.04 ± 0.03 | 0.703 ± 0.012 | 9 ± 5 | −2.2 ± 1.1 |
| | Fibrous fringe | 4 | −15.68 ± 0.09 | −0.70 ± 0.02 | 0.673 ± 0.012 | 18 ± 5 | 0.1 ± 1.1 |
| | Spar | 4 | −10.69 ± 0.11 | −10.74 ± 0.07 | 0.677 ± 0.011 | 17 ± 5 | −10.1 ± 1.0 |
| 161a | Body | 4 | −17.34 ± 0.05 | −0.89 ± 0.03 | 0.690 ± 0.011 | 13 ± 5 | −1.2 ± 1.0 |
| | Inner fibrous fringe | 3 | −16.81 ± 0.11 | −0.27 ± 0.03 | 0.677 ± 0.013 | 17 ± 5 | 0.3 ± 1.2 |
| | Outer fibrous fringe | 4 | 1.66 ± 0.09 | −0.93 ± 0.02 | 0.654 ± 0.012 | 24 ± 5 | 1.2 ± 1.1 |
| | Spar | 4 | −5.62 ± 0.11 | −11.74 ± 0.07 | 0.653 ± 0.011 | 25 ± 5 | −9.5 ± 1.1 |
| SC8 | Body | 5 | −14.89 ± 0.04 | −0.75 ± 0.02 | 0.658 ± 0.009 | 23 ± 5 | 1.2 ± 1.0 |
| | Inner fibrous fringe | 3 | −14.95 ± 0.11 | −0.30 ± 0.03 | 0.677 ± 0.013 | 17 ± 5 | 0.3 ± 1.2 |
| | Outer fibrous fringe | 3 | −2.34 ± 0.11 | −0.40 ± 0.03 | 0.629 ± 0.013 | 33 ± 6 | 3.5 ± 1.2 |
| | Spar | 5 | −7.46 ± 0.10 | −3.38 ± 0.07 | 0.672 ± 0.010 | 18 ± 5 | −2.5 ± 1.0 |
| Ampthill Clay, Peterborough[c] | | | | | | | |
| P35-95 | Body | 3 | −19.50 ± 0.06 | −0.70 ± 0.03 | 0.683 ± 0.012 | 15 ± 5 | −0.5 ± 1.1 |
| | Inner fibrous fringe | 3 | −19.80 ± 0.11 | −0.68 ± 0.03 | 0.683 ± 0.013 | 15 ± 5 | −0.5 ± 1.1 |
| | Outer fibrous fringe | 4 | −20.10 ± 0.09 | −1.21 ± 0.02 | 0.670 ± 0.012 | 19 ± 5 | −0.1 ± 1.1 |
| | Spar | 3 | −0.47 ± 0.13 | −9.55 ± 0.08 | 0.630 ± 0.013 | 33 ± 6 | −5.7 ± 1.2 |
| Oxford Clay, Peterborough[c] | | | | | | | |
| P1A-B | Body | 3 | −15.69 ± 0.06 | −0.80 ± 0.03 | 0.697 ± 0.012 | 11 ± 5 | −1.5 ± 1.1 |
| | Spar | 4 | −0.15 ± 0.11 | −9.53 ± 0.07 | 0.602 ± 0.011 | 43 ± 6 | −3.7 ± 1.1 |
| | Spar | 3[d] | −0.16 ± 0.14 | −9.52 ± 0.09 | 0.616 ± 0.011 | 38 ± 6 | −4.7 ± 1.1 |
| Oxford Clay, Calvert[e] | | | | | | | |
| C5 | Body | 3 | −14.25 ± 0.06 | −0.66 ± 0.03 | 0.673 ± 0.012 | 18 ± 5 | 0.2 ± 1.1 |
| | Spar | 3 | −0.41 ± 0.13 | −7.34 ± 0.08 | 0.638 ± 0.013 | 30 ± 6 | −4.1 ± 1.2 |
| Oxford Clay, Cassington[f] | | | | | | | |
| CAS1095-6 | Body | 3 | −14.72 ± 0.06 | −0.76 ± 0.03 | 0.675 ± 0.012 | 17 ± 5 | 0.0 ± 1.1 |
| | Spar | 3 | 0.86 ± 0.13 | −7.93 ± 0.08 | 0.650 ± 0.013 | 26 ± 6 | −5.5 ± 1.1 |

*Note:* All ± values represent one standard error of the pooled standard deviation.

[a]CDES is Carbon Dioxide Equilibrium Scale.

[b]Location: 57.661774 −6.246455 (WGS84).

[c]Location: 52.509702 −0.274535 (WGS84).

[d]Same sample as above, excluding one high-temperature measurement; see text.

[e]Location: 51.903016 −0.991232 (WGS84).

[f]Location: 51.794775 −1.318454 (WGS84).

The brown fibrous cement fringes mostly gave temperatures between 15 ± 5°C and 19 ± 5°C, and pore fluid values between −0.5 ± 1.1‰ and 0.3 ± 1.2‰$_{VSMOW}$ (Figure 3C). Two Skye concretions with thick fibrous calcite fringes that were sub-sampled (Figure 3A and Supplemental Information) display increasing temperatures and more $^{18}O$-enriched pore fluid compositions from the inner to outer edges (Table 1).

Temperatures and pore fluid compositions for void-filling spars are variable in both geographic regions (Figure 3C), 151-7 (Skye) having the lowest (17 ± 5°C) and P1A-B (Peterborough) the highest at 43 ± 6°C. Spars from the Oxford and Ampthill Clays gave fluid compositions between −3.7 ± 1.1‰ and −5.7 ± 1.2‰$_{VSMOW}$, whereas two concretions from the Staffin Shale had spar fluid compositions of −10.1 ± 1.0‰ and −9.5 ± 1.1‰$_{VSMOW}$. SC8 (Skye) was again an exception, with a pore fluid value of −2.5 ± 1.0‰$_{VSMOW}$.

## 4 | INTERPRETATION AND DISCUSSION

The variances of individual sample replicates (see Supplemental Information) are typically close to, or less than the overall pooled uncertainties, are similar between different

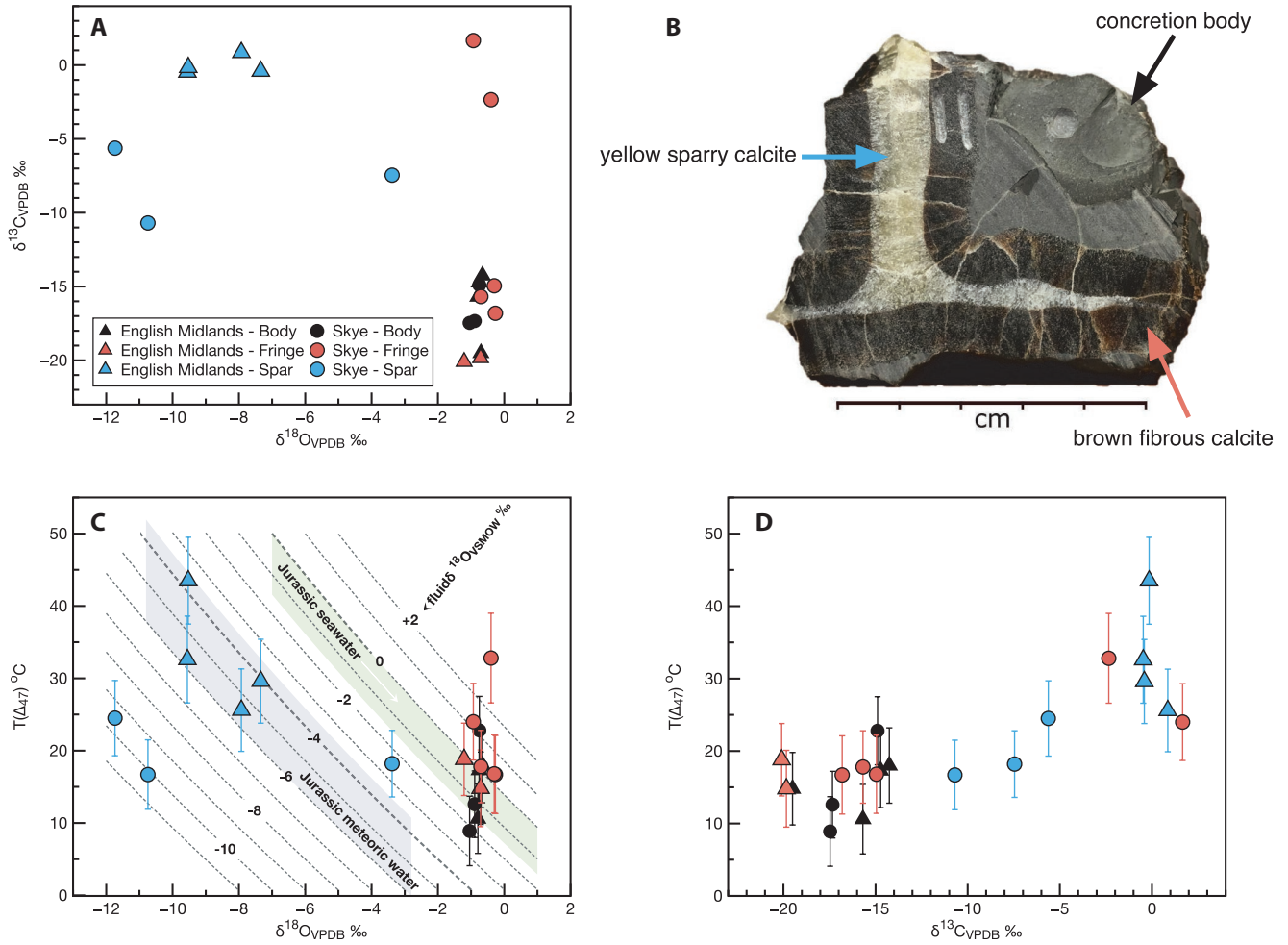


**FIGURE 3** Cross plots of geochemical and $\Delta_{47}$ temperature data showing (A) stable isotope data; (B) sample pits and calcite phases of sample SC8; (C) $\Delta_{47}$ temperature data vs $\delta^{18}O$ and; (D) $\Delta_{47}$ temperature data vs $\delta^{13}C$. Error bars represent one standard error of the pooled standard deviation (see Table 1). The $\delta^{18}O_{VPDB}$ and $\delta^{13}C_{VPDB}$ errors are <symbol dimensions

calcite phases, and are also commensurate with the long-term uncertainty associated with measurement of the standards. This statistical information indicates that sampling resulted in homogeneous powders for analysis. However, it is possible that some of the sample internal variance might reflect original inhomogeneity in the sediments including minor variation in the timing of cementation of residual porosity in the concretion bodies. There is no petrographic evidence to suggest the latter is probable in these sampled concretions (Hendry et al., 2006; Hudson et al., 2001) although electron backscatter data in Loyd et al. (2014) imply <10% 'pseudospar' patches in some of their British concretion bodies. Other causes of variance could be due to inclusion of undetected cements in microfractures and the possibility of crystal face disequilibrium effects (Dickson, 1991) in the coarser sparry calcites. However, the simple mixing modelling (Supplemental Information, section 5) proposed here indicates that all phase mixing can be excluded other than a very small fraction of spar cement.

For most concretions, the clumped isotope data from the earliest-formed calcites (body, cement fringe) gave temperatures between 9 ± 5°C and 19 ± 5°C (Table 1). In addition, all but one concretion body sample (151-7 from Staffin; Table 1) gave derived water $\delta^{18}O$ values of *ca* $-1‰_{VSMOW}$ $\delta^{18}O$, consistent with the values for Jurassic sea water proposed by Shackleton and Kennett (1975). The data thus indicate calcite precipitation from marine pore fluids, consistent with the Sr isotope compositions (Hudson et al., 2001). There is little evidence that the concretion bodies were pervasively altered by meteoric waters (cf. Mozley & Burns, 1993) and no evidence for pervasive alteration by a secondary phase of hot (33–46°C) $^{18}O$-enriched pore water, which Loyd et al. (2014) proposed for some of the same material.

Taken together the concretion body results are a new measure of mean bottom water temperatures of *ca* 15°C (range 9–18°C) in British Callovian-Kimmerdigian seas, in agreement with earlier Callovian benthic (Hudson et al., 2001; Mettam et al., 2014) and Kimmeridgian water column (belemnite rostra $\delta^{18}O$, Staffin Shale Formation) temperature estimates between 14 and <20°C (Nunn et al., 2009; Wierzbowski et al., 2006). Moreover, these abiogenic concretion body

calcites are probably a more secure guide to bottom water temperatures than fossil skeletal carbonates because assumptions about biogenic vital effects are not required. In this context, note both the high variability in $\delta^{18}O$ values from Staffin Shale Formation belemnite rostra (Nunn et al., 2009; Wierzbowski et al., 2006) and their remarkably high clumped isotope temperatures (Vickers et al., 2020), suggesting undetected disequilibrium effects. Only the coolest belemnite apical-line clumped isotope temperature of 18.7 ± 5°C, thought to reflect benthic or synsedimentary conditions in the Staffin Shale Formation (Vickers et al., 2020), overlaps the concretion body temperature range reported here.

These results align well with established views that British Jurassic concretion body calcites precipitated under very shallow marine burial conditions (Hendry et al., 2006; Hudson, 1978; Hudson et al., 2001; Raiswell, 1976) within the BSR zone, as supported by negative $\delta^{13}C$ compositions (Figure 3D; see also Hudson et al., 2001; Irwin et al., 1977; Mozley & Burns, 1993). The similarity of the data from the concretion bodies and the fracture-hosted fibrous cement fringes also support the inference that septarian fracture initiation and subsequent fringe cementation were penecontemporaneous with formation of the concretion body under marine shallow burial conditions (Hendry et al., 2006; Hudson et al., 2001).

The rates of crystallization of these earliest-formed calcite phases are not known so assumptions regarding isotopic equilibrium are difficult to substantiate. This noted, it is striking that the clumped isotope temperatures are consistent with the wider geological context of concretion growth (Hendry et al., 2006; Hudson, 1978; Sellés-Martínez, 1996), suggesting that they did form under near isotopic equilibrium.

In most cases the fibrous cement fringes formed from sea water-derived pore fluids between 4 and 9°C warmer than the fluid from which the concretion bodies formed. Sub-samples of a cement fringe from the Ampthill Clay concretion did not record significant changes in temperature or fluid composition from inner to outer edge (Table 1). However, two concretions from the Staffin Shale of Skye both show a transition from initial precipitation at 17 ± 5°C from pore fluids with a $\delta^{18}O$ value of 0.3 ± 1.2‰, to significantly warmer temperatures and slightly more evolved pore fluids close to the outer edge of the cement (Table 1). These data are consistent with initial growth at shallow burial within, and perhaps near the base, of the BSR zone (Hendry et al., 2006), followed by deeper burial (warmer pore water) and transition beyond the BSR zone, as suggested by gradually increasing $\delta^{13}C$ values (Hendry et al., 2006). The enrichment of $^{18}O$ in these Staffin Shale fluids (Table 1) suggests some near-closed system, water/sediment interaction; limited reaction with a silicic sediment component like volcanic ash (Knox, 1977) would achieve this (cf. Noh & Lee, 1999). It is noteworthy that the $^{18}O$ enrichment and temperature increase have opposing effects on the $\delta^{18}O_{carbonate}$ value (Table 1), such that without $\Delta_{47}$ data little if any change in the conditions of precipitation would be apparent.

Sparry calcites that partially or wholly fill void spaces are the final carbonate cement phases in all the studied concretions. Clumped isotope temperatures for these cements are variable (from 26 ± 6°C to 43 ± 6°C for the English concretions; and 17 ± 5°C to 25 ± 5°C from the Skye concretions; Table 1), but usually higher than the corresponding concretion body temperature, consistent with formation under relatively deeper burial. The Oxford and Ampthill Clay spars precipitated from pore fluids with $\delta^{18}O$ values between −3.7 ± 1.1‰ and −5.7 ± 1.2‰$_{VSMOW}$, while spars in two of the Skye concretions precipitated from fluids with $\delta^{18}O$ values between −9.5 ± 1.1‰ and −10.1 ± 1.0‰$_{VSMOW}$ (Table 1). These fluid compositions indicate the presence of meteoric waters, confirming conclusions of earlier studies (Hendry et al., 2006; Hudson, 1978; Hudson et al., 2001; Loyd et al., 2014).

In one Skye concretion (SC8), the fringe cement data are comparable with other concretions in this study but the body yielded a temperature of 23 ± 5°C (Table 1), warmer than any of the others. As the SC8 $\delta^{18}O$ value is not anomalous, it is suggested that the higher temperature results from disequilibrium effects on $\Delta_{47}$. In addition, while the spar from SC8 had a comparable precipitation temperature (18 ± 5°C) to that of other concretions, the derived pore water composition was much more $^{18}O$-enriched (−2.5 ± 1.0‰$_{VSMOW}$ compared to between −9.5 ± 1.1‰ and −10.1 ± 1.0‰$_{VSMOW}$ for the other Skye concretions; Table 1). The reason for this difference is not clear; however, Hendry et al. (2006) recorded a large range in Staffin Shale concretion sparry calcite $\delta^{18}O_{carbonate}$, ranging from −1.5‰ to −17‰$_{VPDB}$, suggesting substantial heterogeneity in pore fluid composition between concretions. This variation might be due to spars precipitating from fluids at different stages of burial and uplift, including progressive displacement by Palaeocene meteoric water (Hendry et al., 2006).

The clumped isotope temperatures for all concretion calcite phases are below the maximum burial temperature estimates for their locations (<60°C for the Staffin Shale; Lefort et al., 2012; Pearson et al., 2005; Vickers et al., 2020; ≤50°C for Southern England; Green et al., 2001). The highest temperature measured (43 ± 6°C) was for a spar from P1A-B. This value is a mean of four repeats, one of which gave much higher temperatures (Table 1); excluding this outlier gives a temperature of 38 ± 6°C and a fluid $\delta^{18}O$ composition of −4.7 ± 1.1‰$_{VSMOW}$ (Table 1), more in line with data from the other English concretions. However, since there is no evidence for contamination at mass 48 in this outlier, all the data in the mean temperature reported are retained.

The clumped isotope temperatures reported here from sparry fracture fills are similar to those of Loyd et al. (2014); they report temperatures of 32 ± 2 to 48 ± 2°C from Oxford and Ampthill Clay spars. However, Loyd et al. (2014) also report elevated temperatures for the earlier diagenetic phases

(body, cement fringe); in contrast this study shows that the earlier cements were precipitated at, or close to Earth surface temperatures. This difference is clear in the reported $\Delta_{47}$ values (Figure 4). There are a number of factors, mostly methodological, that may account for this difference, which are explored below.

The most obvious difference between the spars and the earlier diagenetic phases is a *ca* 15‰ depletion in $\delta^{13}C$ values for the Oxford and Ampthill Clay concretions body cements (−14.3 to −19.5‰$_{VPDB}$) when compared to the spars (0.9 to −0.5‰$_{VPDB}$). As has been shown by Schauer et al. (2016) and Daëron et al. (2016) there is a subtle but significant effect of the $^{17}O$ correction algorithm on reported $\Delta_{47}$ values when using different values for $R^{17}{}_{VSMOW}$ and $\lambda$, the gradient of the oxygen isotope mass dependent fractionation line. Early studies typically used values of $R^{17}{}_{VSMOW} = 0.0003799$ and $\lambda = 0.5164$. Using these values, concretion body cement samples with depleted $\delta^{13}C$ values compared to spar cements will record $\Delta_{47}$ values that are too low, and thus higher apparent temperatures. The parameters used in the $^{17}O$ correction algorithm by Loyd et al. (2014) were not reported but, since their work precedes recognition of the importance of parameters employed, it is probable that they are now out-dated.

Other methodological differences between this study and that of Loyd et al. (2014) include the following. (a) The use of different temperature calibrations. Loyd et al. (2014) used the Ghosh et al. (2006) calibration as transformed onto the CDES by Dennis et al. (2011), which is at marked variance with virtually all other published calibrations. (b) Loyd et al. (2014) used the Passey et al. (2010) correction of +0.08‰ $\Delta_{47}$ in order to correct their results to an acid reaction temperature of 25°C. It is probable that this correction value varies between reaction systems and schemes; for example, a value of +0.062‰ is reported here. (c) A significant correction for linearity is required in the Loyd et al. (2014) study. Since there is a large difference in the $\delta_{47}$ value of body and spar cements then small errors in the linearity correction will translate into variable offsets of the reported true $\Delta_{47}$ value as a function of the bulk $\delta_{47}$ value. It is probable that a contribution of one, or more of these methodological factors can explain the apparent elevated body cement temperatures reported by Loyd et al. (2014) when compared to the data reported here.

Additionally, there are possible effects associated with sample mineralogy and organic matter content, as well as possible mixing effects. The major difference between the spars and the earlier diagenetic phases (body, cement fringe) is that spars are largely free of non-carbonate impurities. In comparison, the concretion body cements have cemented pore space in host shales that include siliciclastic minerals, organic matter and pyrite framboids (Hendry et al., 2006; Hudson, 1978), while the early fibrous fringes contain abundant high molecular weight organic inclusions

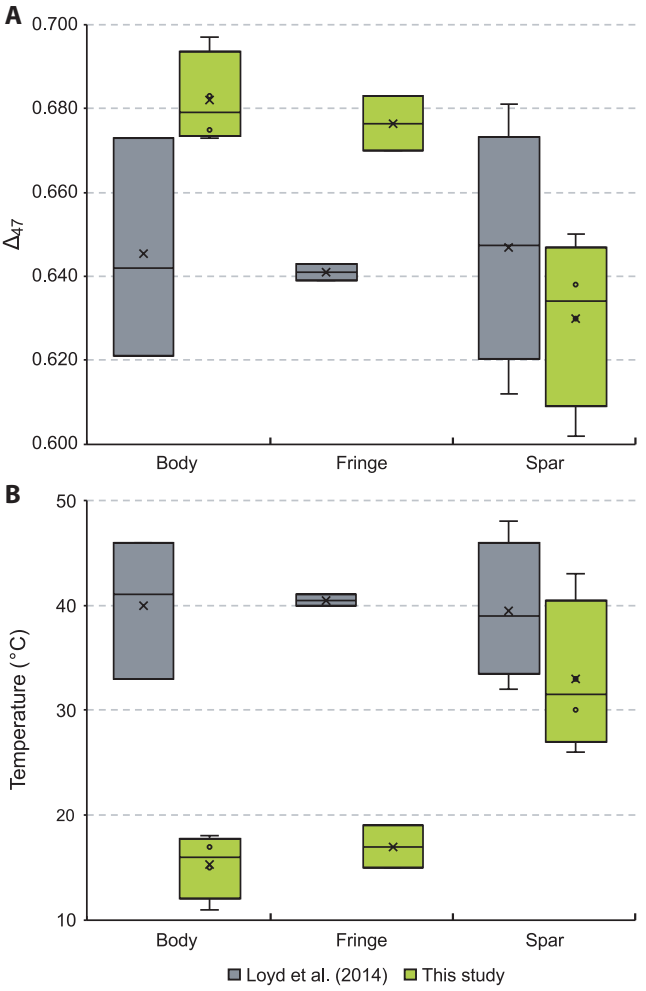


**FIGURE 4** Box and whisker diagram of: (A) $\Delta_{47}$ values and (B) temperatures reported for body, fringe and spar cements of Oxford and Ampthill Clay concretions by Loyd et al. (2014) and this study

(Pearson et al., 2005). It is thus possible that non-carbonate derived contaminant molecules at the cardinal masses of the $CO_2$ isotopologues could cause inter-laboratory differences in results from impure carbonate samples. In the authors' experience, such contamination invariably leads to elevated $\Delta_{48}$ and $\Delta_{47}$ values and the reporting of too low a temperature. The data in Loyd et al. (2014) are not consistent with this observation as they show body cements precipitated at similar temperatures to the spar cements (see Figure 4). However, contaminants at masses 46 and 48 have been reported to lead to a lowered $\Delta_{47}$ and too high apparent temperatures (Snell et al., 2019). Potential contaminants include $NO_2$ arising from ammonium adsorbed on clay particles which has been previously identified as causing significant shifts in measured $\delta^{18}O$ ($\delta_{46}$) values of carbonate cements (Mucciarone & Williams, 1990).

An additional effect may be caused by the mixing of cement phases (see Supplemental Information). It is possible to include a component of spar cement when sampling concretion body cements if small veins of microspar are not

identified. Mixing of these two phases can lead to lowered $\Delta_{47}$ and higher apparent temperatures. Note, however, that Loyd et al. (2014) report taking great care during sampling to avoid mixing of phases.

Ultimately, it is thought most probable that the methodological differences between this study and that of Loyd et al. (2014), notably the $^{17}O$ correction, go a long way to explaining the different conclusions regarding the comparative temperatures of concretion body and spar cements. The differences in data and interpretation are entirely understandable given the still novel nature of the clumped isotope method and the on-going rapid development of the technique. As clumped isotope mass spectrometry evolves, and the understanding of the subtleties improves, convergence of results should follow.

## 5 | CONCLUSIONS

New clumped isotope data from British Jurassic septarian concretions demonstrate:

1. That earliest-formed (synsedimentary) concretion body calcites mostly precipitated at temperatures between 9 ± 5°C and 18 ± 5°C, from fluids with $\delta^{18}O$ values between 0.2 ± 1.1‰ and −2.2 ± 1.1‰$_{VSMOW}$. The fluid compositions indicate Jurassic sea water and the temperatures are recording bottom water/in-sediment conditions.
2. Early diagenetic, brown, fibrous cement fringes mostly gave temperatures between 15 ± 5°C and 19 ± 5°C, and pore fluid values between −0.5 ± 1.1‰ and 0.3 ± 1.2‰$_{VSMOW}$. These results again imply a marine fluid under very shallow burial conditions.
3. Later diagenetic sparry calcite cements formed between 17 ± 5°C and 43 ± 6°C with fluid compositions between −2.5 ± 1.0‰ and −10.1 ± 1.0‰$_{VSMOW}$, indicating precipitation from meteoric-influenced fluids under shallow burial conditions.

These data are consistent with established views on the formation of Jurassic septarian concretions and also demonstrate their potential to provide robust sea floor palaeotemperatures, free from assumptions about 'vital effects' associated with biogenic carbonates. While the data on early diagenetic phases presented in this study differ from an earlier clumped isotope study on similar concretions (Loyd et al., 2014), the disparity is probably caused by methodological differences.

## ACKNOWLEDGEMENTS

The authors thank Amber Vaughan (then UEA) for pilot clumped isotope work on Jurassic concretions and Tim Atkinson (UCL) for field support. RP is supported by the Natural Environment Research Council through the EnvEast Doctoral Training Partnership (NE/L002582/1). Jim Marshall and an anonymous reviewer gave helpful comments that stimulated better understanding of the data.

## DATA AVAILABILITY STATEMENT

Supplemental Information, including a file of all data, is included with this manuscript and is openly available in 'figshare' at https://doi.org/10.6084/m9.figshare.13567667.v2. The data that support the findings of this study will also be openly available in the future in the NERC Data Centre 'National Geoscience Data Centre'.

## ORCID

*Richmal B. Paxton* https://orcid.org/0000-0002-3987-6670

## REFERENCES

Bernasconi, S.M., Müller, I.A., Bergmann, K.D., Breitenbach, S.F., Fernandez, A., Hodell, D.A. et al. (2018) Reducing uncertainties in carbonate clumped isotope analysis through consistent carbonate-based standardization. *Geochemistry, Geophysics, Geosystems*, *19* (9), 2895–2914. https://doi.org/10.1029/2017GC007385

Cox, B., Gallois, R. & Sumbler, M. (1994) The stratigraphy of the BGS Hartwell borehole, near Aylesbury, Buckinghamshire. *Proceedings of the Geologists' Association*, *105*(3), 209–224. https://doi.org/10.1016/S0016-7878(08)80120-4

Daëron, M., Blamart, D., Peral, M. & Affek, H.p. (2016) Absolute isotopic abundance ratios and the accuracy of Δ47 measurements. *Chemical Geology*, *442*, 83–96. https://doi.org/10.1016/j.chemgeo.2016.08.014

Daëron, M., Drysdale, R.N., Peral, M., Huyghe, D., Blamart, D., Coplen, T.B. et al. (2019) Most earth-surface calcites precipitate out of isotopic equilibrium. *Nature Communications*, *10*(1), 1–7. https://doi.org/10.1038/s41467-019-08336-5

Dale, A., John, C.M., Mozley, P.S., Smalley, P. & Muggeridge, A.H. (2014) Time-capsule concretions: Unlocking burial diagenetic processes in the Mancos Shale using carbonate clumped isotopes. *Earth and Planetary Science Letters*, *394*, 30–37.10.1016/j.epsl.2014.03.004

De Craen, M., Swennen, R., Keppens, E., Macaulay, C. & Kiriakoulakis, K. (1999) Bacterially mediated formation of carbonate concretions in the Oligocene Boom Clay of northern Belgium. *Journal of Sedimentary Research*, *69*(5), 1098–1106. https://doi.org/10.2110/jsr.69.1098

Defliese, W.F. & Lohmann, K.C. (2016) Evaluation of meteoric calcite cements as a proxy material for mass-47 clumped isotope thermometry. *Geochimica et Cosmochimica Acta*, *173*, 126–141. https://doi.org/10.1016/j.gca.2015.10.022

Dennis, K.J., Affek, H.P., Passey, B.H., Schrag, D.P. & Eiler, J.M. (2011) Defining an absolute reference frame for 'clumped' isotope studies of CO2. *Geochimica et Cosmochimica Acta*, *75*(22), 7117–7131. https://doi.org/10.1016/j.gca.2011.09.025

Dennis, P.F., Myhill, D.J., Marca, A. & Kirk, R. (2019) Clumped isotope evidence for episodic, rapid flow of fluids in a mineralized fault system in the Peak District, UK. *Journal of the Geological Society*, *176*(3), 447–461. https://doi.org/10.1144/jgs2016-117

Dickson, J.A.D. (1991) Disequilibrium carbon and oxygen isotope variations in natural calcite. *Nature*, *353*(6347), 842–844. https://doi.org/10.1038/353842a0

Duff, D. (1975) Paleoecology of a bituminous shale–The Lower Oxford Clay of central England. *Paleontology*, *18*, 443–482.

Eiler, J.M. (2007) "Clumped-isotope" geochemistry—The study of naturally-occurring, multiply-substituted isotopologues. *Earth and Planetary Science Letters*, *262*(3–4), 309–327. https://doi.org/10.1016/j.epsl.2007.08.020

Eiler, J.M. (2011) Paleoclimate reconstruction using carbonate clumped isotope thermometry. *Quaternary Science Reviews*, *30*(25-26), 3575–3588. https://doi.org/10.1016/j.quascirev.2011.09.001

Ghosh, P., Adkins, J., Affek, H., Balta, B., Guo, W., Schauble, E.A. et al. (2006) 13C–18O bonds in carbonate minerals: A new kind of paleothermometer. *Geochimica et Cosmochimica Acta*, *70*(6), 1439–1456. https://doi.org/10.1016/j.gca.2005.11.014

Green, P.F., Thomson, K. & Hudson, J.D. (2001) Recognition of tectonic events in undeformed regions: Contrasting results from the Midland Platform and East Midlands Shelf, Central England. *Journal of the Geological Society*, *158*(1), 59–73. https://doi.org/10.1144/jgs.158.1.59

Hendry, J.P., Pearson, M.J., Trewin, N.H. & Fallick, A.E. (2006) Jurassic septarian concretions from NW Scotland record interdependent bacterial, physical and chemical processes of marine mudrock diagenesis. *Sedimentology*, *53*(3), 537–565. https://doi.org/10.1111/j.1365-3091.2006.00779.x

Hudson, J. (1978) Concretions, isotopes, and the diagenetic history of the Oxford Clay (Jurassic) of central England. *Sedimentology*, *25*(3), 339–370. https://doi.org/10.1111/j.1365-3091.1978.tb00317.x

Hudson, J., Coleman, M., Barreiro, B. & Hollingworth, N. (2001) Septarian concretions from the Oxford Clay (Jurassic, England, UK): Involvement of original marine and multiple external pore fluids. *Sedimentology*, *48*(3), 507–531. https://doi.org/10.1046/j.1365-3091.2001.00374.x

Huntington, K.W., Budd, D.A., Wernicke, B.P. & Eiler, J.M. (2011) Use of clumped-isotope thermometry to constrain the crystallization temperature of diagenetic calcite. *Journal of Sedimentary Research*, *81*(9), 656–669. https://doi.org/10.2110/jsr.2011.51

Irwin, H., Curtis, C. & Coleman, M. (1977) Isotopic evidence for source of diagenetic carbonates formed during burial of organic-rich sediments. *Nature*, *269*(5625), 209–213. https://doi.org/10.1038/269209a0

Kenig, F., Hayes, J., Popp, B. & Summons, R. (1994) Isotopic biogeochemistry of the Oxford Clay Formation (Jurassic), UK. *Journal of the Geological Society*, *151*(1), 139–152. https://doi.org/10.1144/gsjgs.151.1.0139

Kim, S.-T. & O'Neil, J.R. (1997) Equilibrium and nonequilibrium oxygen isotope effects in synthetic carbonates. *Geochimica et Cosmochimica Acta*, *61*(16), 3461–3475. https://doi.org/10.1016/S0016-7037(97)00169-5

Kirk, R. (2017) Development of clumped isotope techniques and their application to palaeoclimate studies. PhD thesis, University of East Anglia.

Knox, R.O.B. (1977) Upper Jurassic pyroclastic rocks in Skye, west Scotland. *Nature*, *265*(5592), 323–324. https://doi.org/10.1038/265323a0

Lefort, A., Hautevelle, Y., Lathuilière, B. & Huault, V. (2012) Molecular organic geochemistry of a proposed stratotype for the Oxfordian/Kimmeridgian boundary (Isle of Skye, Scotland). *Geological Magazine*, *149*(5), 857–874. https://doi.org/10.1017/S0016756811001117

Loyd, S.J., Corsetti, F.A., Eiler, J.M. & Tripati, A.K. (2012) Determining the diagenetic conditions of concretion formation: Assessing temperatures and pore waters using clumped isotopes. *Journal of Sedimentary Research*, *82*(12), 1006–1016. https://doi.org/10.2110/jsr.2012.85

Loyd, S.J., Dickson, J., Boles, J.R. & Tripati, A.K. (2014) Clumped-isotope constraints on cement paragenesis in septarian concretions. *Journal of Sedimentary Research*, *84*(12), 1170–1184. https://doi.org/10.2110/jsr.2014.91

Mettam, C., Johnson, A.L., Nunn, E.V. & Schöne, B.R. (2014) Stable isotope (δ18O and δ13C) sclerochronology of Callovian (Middle Jurassic) bivalves (Gryphaea (Bilobissa) dilobotes) and belemnites (*Cylindroteuthis puzosiana*) from the Peterborough Member of the Oxford Clay Formation (Cambridgeshire, England): Evidence of palaeoclimate, water depth and belemnite behaviour. *Palaeogeography, Palaeoclimatology, Palaeoecology*, *399*, 187–201. https://doi.org/10.1016/j.palaeo.2014.01.010

Mozley, P.S. & Burns, S.J. (1993) Oxygen and carbon isotopic composition of marine carbonate concretions: An overview. *Journal of Sedimentary Research*, *63*(1), 73–83. https://doi.org/10.1306/D4267A91-2B26-11D7-8648000102C1865D

Mucciarone, D.A. & Williams, D.F. (1990). Stable isotope analyses of carbonate complicated by nitrogen oxide contamination: A delaware Basin example. *Journal of Sedimentary Research*, *60* (4), 608–614. https://doi.org/10.1306/212F91FB-2B24-11D7-8648000102C1865D

Noh, J.H. & Lee, I. (1999) Diagenetic pore fluid evolution in the Pohang Miocene sediments: Oxygen isotopic evidence of septarian carbonate concretions and authigenic mineral phases. *Geosciences Journal*, *3*(3), 141–149. https://doi.org/10.1007/BF02910270

Nunn, E.V., Price, G.D., Hart, M.B., Page, K.N. & Leng, M.J. (2009) Isotopic signals from Callovian-Kimmeridgian (Middle–Upper Jurassic) belemnites and bulk organic carbon, Staffin Bay, Isle of Skye, Scotland. *Journal of the Geological Society*, *166*(4), 633–641. https://doi.org/10.1144/0016-76492008-067

Passey, B.H., Levin, N.E., Cerling, T.E., Brown, F.H. & Eiler, J.M. (2010). High-temperature environments of human evolution in East Africa based on bond ordering in paleosol carbonates. *Proceedings of the National Academy of Sciences of the USA*, *107*(25), 11245–11249. https://doi.org/10.1073/pnas.1001824107

Pearson, M., Hendry, J., Taylor, C. & Russell, M. (2005) Fatty acids in sparry calcite fracture fills and microsparite cement of septarian diagenetic concretions. *Geochimica et Cosmochimica Acta*, *69*(7), 1773–1786. https://doi.org/10.1016/j.gca.2004.09.024

Purvis, K., Dennis, P., Holt, L. & Marca, A. (2020) The origin of carbonate cements in the hildasay reservoir, Cambo Field, Faroe-Shetland Basin: Clumped isotopic analysis and implications for reservoir performance. *Marine and Petroleum Geology*, *122*, 104641. https://doi.org/10.1016/j.marpetgeo.2020.104641

Raiswell, R. (1976) The microbiological formation of carbonate concretions in the Upper Lias of NE England. *Chemical Geology*, *18*(3), 227–244. https://doi.org/10.1016/0009-2541(76)90006-1

Raiswell, R. & Fisher, Q. (2000) Mudrock-hosted carbonate concretions: A review of growth mechanisms and their influence on chemical and isotopic composition. *Journal of the Geological Society*, *157*(1), 239–251. https://doi.org/10.1144/jgs.157.1.239

Schauer, A.J., Kelson, J., Saenger, C. & Huntington, K.W. (2016) Choice of correction affects clumped isotope ($\Delta_{47}$) values of $CO_2$ measured with mass spectrometry. *Rapid Communications in Mass Spectrometry*, *30*, 2607–2616. https://doi.org/10.1002/rcm.7743

Sellés-Martínez, J. (1996) Concretion morphology, classification and genesis. *Earth-Science Reviews*, *41*(3–4), 177–210. https://doi.org/10.1016/S0012-8252(96)00022-0

Shackleton, N. & Kennett, J. (1975) Paleotemperature history of the Cenozoic and the initial of Antarctic glaciation: Oxygen and carbon isotope analyses in Deep Sea Drilling Project Sites 277, 279, and 181. *DSDP*, *29*, 599–612.

Snell, K.E., Passey, B.H., Bergmann, K.D. & Davidheiser-Kroll, B. (2019) How contaminants affect accurate measurement of clumped isotopes in CO2. 7th International Clumped Isotope Workshop, Long Beach CA, Oral Presentation.

Vickers, M.L., Fernandez, A., Hesselbo, S.P., Price, G.D., Bernasconi, S.M., Lode, S. et al. (2020) Unravelling Middle to Late Jurassic palaeoceanographic and palaeoclimatic signals in the Hebrides Basin using belemnite clumped isotope thermometry. *Earth and Planetary Science Letters*, *546*, 116401. https://doi.org/10.1016/j.epsl.2020.116401

Wierzbowski, A., Coe, A.L., Hounslow, M.W., Matyja, B.A., Ogg, J.G., Page, K.N. et al. (2006) A potential stratotype for the Oxfordian/Kimmeridgian boundary: Staffin Bay, Isle of Skye, UK. *Volumina Jurassica*, *4*(4), 17–33.

**How to cite this article:** Paxton RB, Dennis PF, Marca AD, Hendry JP, Hudson JD, Andrews JE. Taking the heat out of British Jurassic septarian concretions. *Depositional Rec*. 2021;00:1–11. https://doi.org/10.1002/dep2.139